Electronics and Electrical Engineering

https://www.aimspress.com/journal/ElectrEng

AIMS Electronics and Electrical Engineering, 9(2): 243–259.
DOI: 10.3934/electreng.2025012
Received: 17 February 2025
Revised: 16 April 2025
Accepted: 18 April 2025
Published: 25 April 2025

Research article

A new advanced third-order sliding mode control with adaptive gain adjustment using fuzzy logic technique for standalone photovoltaic systems

Nesrine Cherigui[1,2,*], Abdelkarim Chemidi[1,3], Ahmed Tahour[1] and Mohamed Horch[4]

[1] Ecole supérieure en sciences Appliquées ESSA, Tlemcen 13000, Algeria
[2] Laboratoire d'automatique de Tlemcen
[3] Manufacturing Engineering Laboratory Of Tlemcen
[4] School of Electrical and Energetic Engineering of Oran, 31000, Algeria

* **Correspondence:** Email: Nesrine.cherigui@essa-tlemcen.dz.

Abstract: The nonlinear behavior of photovoltaic (PV) panels, coupled with their strong dependence on atmospheric conditions, necessitates efficient maximum power point tracking (MPPT) techniques to maximize power extraction, reduce costs, and enhance overall system efficiency. The output power of a PV panel is significantly influenced by current-voltage (I-V) and power-voltage (P-V) characteristics, as well as variations in solar irradiance and temperature. Consequently, advanced MPPT control strategies are required to ensure fast transient response, robustness against disturbances, and minimal steady-state oscillations. This paper proposed a novel MPPT strategy based on a fuzzy third-order sliding mode controller (FTOSMC) designed for PV systems. The proposed approach integrated fuzzy logic control (FLC) with third-order sliding mode control (TOSMC) to adaptively adjust control gains in real time, thereby minimizing chattering, improving tracking speed, and disturbances rejection. The effectiveness of the proposed FTOSMC was evaluated through extensive MATLAB/Simulink simulations, comparing its performance against SMC and TOSMC. Simulation results demonstrated that the proposed FTOSMC-based MPPT method outperformed conventional techniques in terms of faster convergence to the maximum power point (MPP), reduced chattering effects, and improved robustness against environmental fluctuations. These advantages made it a promising solution for PV applications, where system stability and energy efficiency were critical concerns.

Keywords: MPPT; fuzzy logic controller; third order sliding mode; photovoltaic system

1. Introduction

Energy plays a crucial role in the economic progress of nations, with oil and gas being the predominant sources that have driven development in recent years. However, reliance on these fossil

fuels has resulted in the emission of toxic gases, contributing to global warming and climate change. As the demand for electricity continues to rise in both industrial and residential sectors, the production of energy predominantly from fossil fuels raises concerns about resource depletion and environmental degradation. This situation underscores the urgent need for alternative energy sources. Renewable energy options such as solar, wind, hydropower, biomass, biofuels, and geothermal offer sustainable solutions that not only meet electricity demands but also reduce pollution and mitigate climate change. Among these alternatives, photovoltaic (PV) systems have gained significant attention due to their numerous advantages, including clean and quiet operation, eco-friendliness, abundance of resources, and zero greenhouse gas emissions. The continuous decrease in production costs for solar cells has further accelerated the adoption of PV systems across both industrial and residential sectors, making them a viable competitor to conventional fossil fuel-based power generation.

PV systems can operate either in grid-connected or standalone configurations. Grid-connected PV systems feed the generated power into the main grid [1, 2], benefiting from grid stability, whereas standalone PV systems function independently, making them ideal for remote areas without access to electricity infrastructure. Unlike grid-connected systems, standalone PV setups must efficiently manage energy storage and power fluctuations, requiring robust control strategies to ensure stable operation. A critical aspect of optimizing standalone PV systems is the implementation of maximum power point tracking (MPPT) techniques [3, 4], which maximize the extracted power under varying environmental conditions.

The photovoltaic system (PVS) exhibits nonlinear behavior under varying environmental conditions, making it essential to employ a nonlinear control strategy for MPPT. A significant body of research has been dedicated to enhancing the energy efficiency of PVSs through the development of techniques for predicting and tracking the optimal operating condition, known as the MPPT. To achieve this goal, a robust control system must continuously monitor and adapt to changes in environmental conditions, ensuring that the system operates at its peak performance. Various MPPT methods have been proposed over the years, including traditional algorithms such as Perturb and Observe (P&O) [5, 6] and Incremental Conductance (INC) [7, 8], which offer simplicity but are sensitive to environmental variations, leading to decreased performance during rapid changes in irradiation or temperature. This sensitivity results in oscillations around the maximum power point, compromising overall system efficiency. Furthermore, traditional controllers often struggle with robustness against external disturbances, making it challenging to accurately regulate output voltage and converter performance. More advanced approaches based on artificial intelligence (AI) [9], such as artificial neural networks [10–12], adaptive neuro-fuzzy inference systems [13, 14], genetic algorithms [15], and particle swarm optimization [16, 17], and the hyperbolic slime mould algorithm (HSMA) [18] have demonstrated high accuracy, stability, and robustness to internal load variations and system parameter changes. These methods offer several advantages, including high efficiency and robustness. However, these methods often require high computational resources, limiting their real-time implementation in embedded systems.

Nonlinear control strategies, particularly sliding mode control (SMC), have emerged as effective alternatives due to their robustness against disturbances and uncertainties. While SMC-based MPPT controllers improve dynamic response and stability [19–22] they are often associated with chattering, phenomenon that can lead to several problems such as efficiency losses and reduced system lifetime. To address this problem, a new nonlinear approach called third-order SMC (TOSMC) has been introduced

as a mitigation strategy [23]. This innovative control strategy demonstrates improved performance by reducing chattering compared to classical SMC methods. Despite its advantages, TOSMC still requires well-tuned parameters to maintain optimal performance under rapidly changing conditions; furthermore, the parameters are fixed. To further enhance the efficiency of TOSMC and mitigate its inherent limitations, in this paper, a novel fuzzy third-order SMC (FTOSMC) strategy is proposed to enhance MPPT performance in standalone PV systems. By integrating fuzzy logic into TOSMC, the gain can be adaptively adjusted in real-time to minimize chattering phenomena and optimize overall system performance.

Compared to conventional MPPT approaches, the proposed FTOSMC method offers several key points:

- **Adaptive Gain Adjustment for Chattering Reduction** – Unlike classical SMC techniques, which suffer from fixed control gains, the fuzzy logic component of FTOSMC ensures adaptive gain tuning, significantly reducing chattering without sacrificing tracking speed.
- **Faster MPPT Convergence** The proposed approach provides a faster response compared to traditional methods such as P&O and INC, enabling efficient power tracking even under rapid changes in irradiance and temperature.
- **Enhanced Robustness to Environmental Disturbances** The ability to dynamically adjust control parameters allows FTOSMC to maintain high efficiency and stability in standalone PV systems, where external disturbances can significantly affect performance.
- **Computational Efficiency for Real-Time Implementation** Unlike AI-based MPPT methods, which require intensive computation, the FTOSMC strategy offers a balance between performance and real-time feasibility, making it suitable for embedded applications.

However, the proposed FTOSMC depends on the proper selection of sliding mode and fuzzy logic parameters.

The proposed FTOSMC strategy is validated through simulations using MATLAB/Simulink environments under various irradiance and temperature profiles. The results demonstrate that FTOSMC outperforms conventional SMC and TOSMC methods in terms of tracking accuracy, chattering reduction, and overall power quality improvement. This paper is organized as follows: Following the introduction, Section 2 offers a concise overview of PVS modeling. Section 3 explores the MPPT using TOSMC. Section 4 introduces the proposed FTOSMC. Section 5 showcases the simulation results, and Section 6 provides the conclusion of the paper.

2. Modeling PV arrays

Solar energy is expected to contribute 20% of the total energy generated, underscoring the growing significance of electricity generation from solar power [22, 24]. One approach to harness electrical energy from solar energy is through semiconductor-based PV arrays. PV solar cells consist of semiconductor materials such as silicon, gallium arsenide, cadmium telluride, or copper indium diselenide, which convert sunlight (photons) directly into electricity. Two common modeling approaches for PV cells are the single diode model and the two diode model. Research indicates that the efficiencies of both models are quite similar under conditions of 25°C. In our study, we employ the single-diode model for the PVS.

The mathematical model, which encompasses the current-voltage relationship, can be readily derived from prior studies.

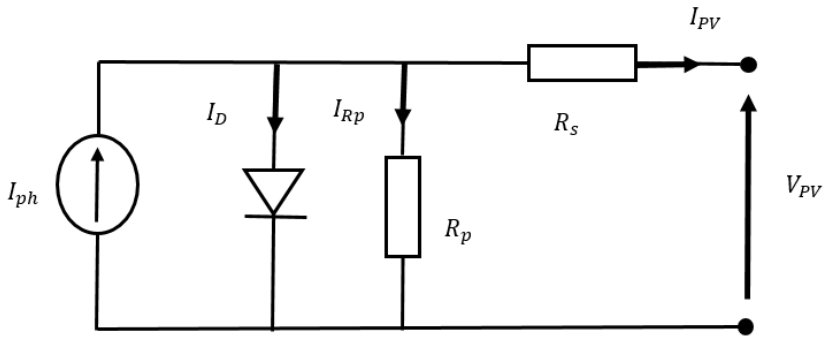

Figure 1. single diode model PV cell.

In this circuit, the current of the PV cell is determined using Equation 2.1 based on fundamental circuit laws.

$$I_{PV} = I_{ph} - I_D - I_{Rp} \tag{2.1}$$

Additionally, the current of an ideal diode can be modeled using the equation expressed in Equation 2.2:

$$I_D = I_s \left[\exp\left(\frac{V_{PV}+I_{PV}R_s}{aV_T}\right) - 1\right] \tag{2.2}$$

The thermal voltage V_T can be calculated using Equation 2.3: where R_s and R_p represent the series and the parallel resistance,respectively. $K = 1.3805.1023j/k$ is the Boltzmann constant, T is the cell temperature, $q = 1.6.1019C$ is the charge of electron, $T_C = 25C$ is the reference temperature (standard conditions), and $a = 1.3$ is the ideality factor of the parallel diode. By applying Equations (2.1)–(2.3) to derive the primary expression for the cell's behavior, we obtain Equation 2.4:

$$V_T = KT_C/q \tag{2.3}$$

$$I_{PV} = I_{ph} - I_D \exp\left(\frac{V_{PV} + I_{PV}R_s}{aV_T}\right) - 1 \tag{2.4}$$

By applying certain assumptions and incorporating the quantities of series cells N_s and parallel cells N_P , Equation 2.5 can be derived:

$$I_{PV} = N_P I_{ph} - N_P I_D \exp\left(\frac{qV_T}{N_s.a.V_T}\right) - 1 \tag{2.5}$$

3. Model of DC-DC boost

The boost chopper (Direct Current-Direct Current) converter circuit is widely utilized due to its familiarity, ease of implementation, and high efficiency. This converter functions to increase the DC voltage applied at its input to a higher level.

The circuit is analyzed in two scenarios based on the state of the switch (Q), either ON or OFF. Consequently, the characteristic equations for the inductor current (I_L) and the output capacitor voltage (V_o) are derived in Equation 3.1:

$$\begin{cases} \frac{dI_L}{dt} = \frac{V_o - V_o}{L} + \frac{V_o}{L}u \\ \frac{dV_O}{dt} = \left(\frac{V_O}{RC} + \frac{I_L}{C}\right) - \frac{I_L}{C}u \end{cases} \tag{3.1}$$

By integrating these equations, the state-space representation of the DC-DC boost converter circuit is derived in matrix form in Equation 3.2, assuming $I_L = I_{PV}$:

$$\frac{d}{dt}\begin{bmatrix} I_{PV} \\ V_O \end{bmatrix} = \begin{bmatrix} 0 & \frac{-1}{L} \\ \frac{1}{C} & \frac{-1}{RC} \end{bmatrix}\begin{bmatrix} I_{PV} \\ V_O \end{bmatrix} + \begin{bmatrix} \frac{V_O}{L} \\ \frac{-I_{PV}}{C} \end{bmatrix} u + \begin{bmatrix} \frac{1}{L} \\ 0 \end{bmatrix} \tag{3.2}$$

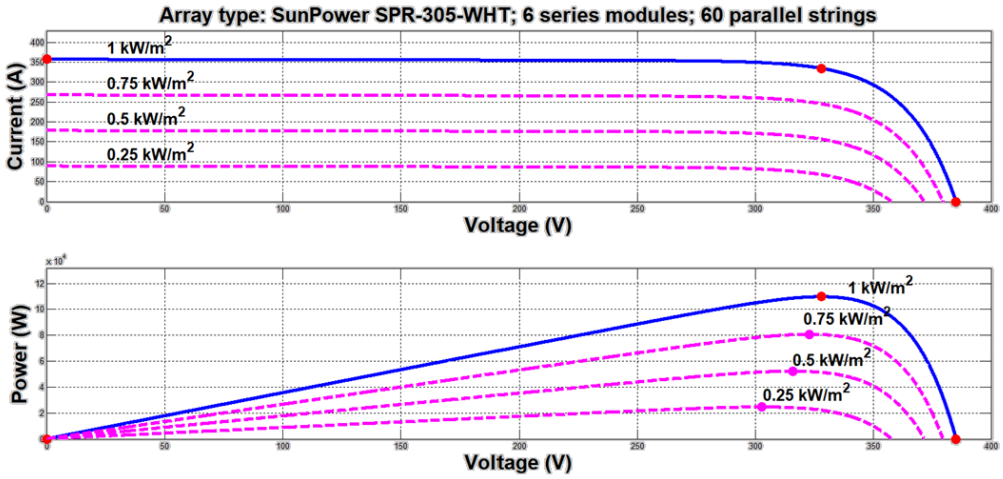

Figure 2. Current-voltage and power-voltage characteristics of PV array under different irradiances.

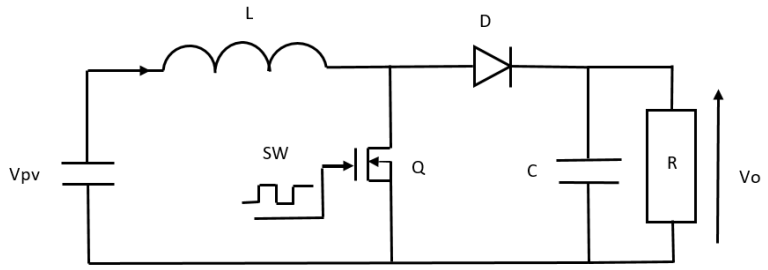

Figure 3. The used boost DC-DC converter circuit.

4. TOSMC

The SMC has been recognized as one of the powerful control strategies for power converters and is commonly employed as a robust control strategy in systems characterized by nonlinearities and parameter uncertainties [23, 25]. A primary challenge associated with SMC in controlling DC-DC

converters is the occurrence of chattering. Although variable switching frequencies can mitigate this issue, researchers typically favor fixed switching frequencies in microcontroller-based applications. In this study, our goal is to achieve MPPT while minimizing chattering. We concentrate on a TOSMC combined with a fuzzy logic controller to optimize power output from the PV panel while reducing chattering. The design of an SMC involves two main steps. The first step is the creation of a sliding surface that guarantees that the operation of the DC-DC converter would be as desired. In the second phase, a control law is created that drives the system onto the sliding surface and keeps it there thereafter. When we define our sliding surface $S(x,t)$, we want it to be zero and we also want its first derivative to be zero.

$$S(X,t) = 0, \dot{S}(X,t) = 0 \tag{4.1}$$

To ensure that the system remains on the sliding surface that yields maximum power, the sliding surface can be expressed as follows:

$$S(X,t) = \frac{\partial P_{PV}}{\partial V_{PV}} = V_{PV}\left(\frac{\partial I_{PV}}{\partial V_{PV}} + \frac{I_{PV}}{V_{PV}}\right) = 0 \tag{4.2}$$

From Equation 3.2, we can write the state–space equation of the boost converter as follows:

$$\dot{X} = f(X) + g(X) * U \tag{4.3}$$

$$\dot{X} = \begin{bmatrix} \frac{dI_{PV}}{dt} \\ \frac{dV_O}{dt} \end{bmatrix} \tag{4.4}$$

$$f(X) = \begin{bmatrix} \frac{V_{PV}-V_O}{L} \\ \frac{I_{PV}}{C} - \frac{V_O}{RC} \end{bmatrix} and g(X) = \begin{bmatrix} \frac{V_O}{L} \\ \frac{-I_{PV}}{C} \end{bmatrix} \tag{4.5}$$

The general control law consists of two components: The first term is for the nonlinear control (U_n), while the second is the equivalent control term (U_{eq}) which is expressed as:

$$U = U_n + U_{eq} \tag{4.6}$$

The control law of the TOSMC algorithm is given as:

$$U_{TOSMC} = (U_1(t) + U_2(t) + U_3(t)) \tag{4.7}$$

where:

$$U_1(t) = \lambda_1 \sqrt{|S|}.sign(S) \tag{4.8}$$

$$U_2(t) = \lambda_2 \int sign(S) \tag{4.9}$$

$$U_3(t) = \lambda_3.sign(S) \tag{4.10}$$

λ_1, λ_2, and λ_3:these are the tuning constants for the TOSMC controller, which offer enhanced flexibility compared to the traditional SMC controller, which uses a single tuning parameter. These parameters will be determined and selected to ensure improved performance of the MPPT technique.

Using Equations (4.3)–(4.5), U_{eq} is obtained as shown in Equation 4.11:

$$U_{eq} = \frac{\left[\frac{\partial S}{\partial X}\right]^T f(X)}{\left[\frac{\partial S}{\partial X}\right]^T g(X)} = 1 - \frac{V_{PV}}{V_O} \tag{4.11}$$

The final formulation of the control signal proposed in this study is provided as follows:

$$U(t) = \lambda_1 \sqrt{|S|}.sign(S) + \lambda_2 \int sign(S).dt + \lambda_3.sign(S) + \left(1 - \frac{V_{PV}}{V_O}\right) \tag{4.12}$$

The next step is to establish the stability of the proposed control approach, which is typically achieved through Lyapunov stability analysis.

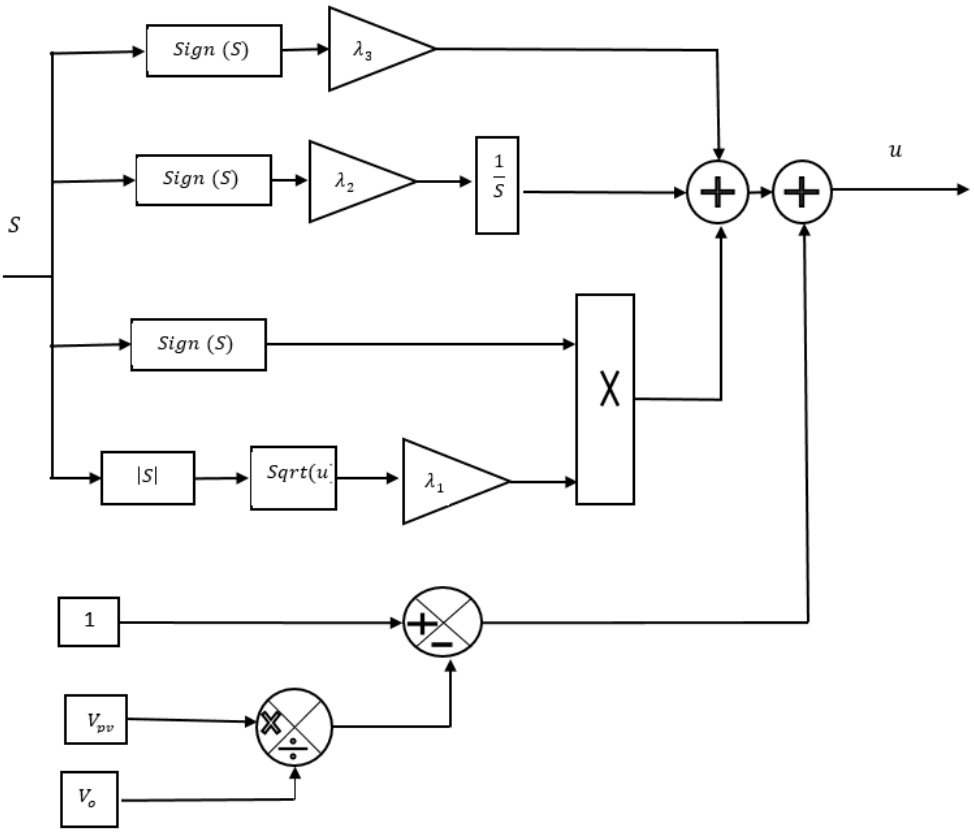

Figure 4. structure of MPPT-based TOSMC algorithm for the PV system.

4.1. Lyapunov stability analysis

Lyapunov stability analysis is a recognized method for assessing the stability of nonlinear systems. This approach involves the use of a selected Lyapunov function $V(X)$ that interacts with the system's dynamics.

The stability of the system is established when the derivative of the Lyapunov function is negative, thereby validating the following conditions:

$$\begin{cases} \dot{V}(t) < 0 \\ S(X) \neq 0 \\ \dot{S}(t) \neq 0 \end{cases} \tag{4.13}$$

A positively defined function $V(X)$ can be chosen based on $S(X,t)$ as:

$$V(X,t) = \frac{1}{2}\left(S(X,t)\right)^2 \tag{4.14}$$

The stability condition in Equation 4.14 can be reformulated as follows:

$$S.\dot{S} < 0 \tag{4.15}$$

The first derivative of the proposed $S(X,t)$ is derived and presented as follows:

$$\dot{S} = \left[\frac{\partial S}{\partial X}\right]^T \dot{X} \tag{4.16}$$

$$\dot{S} = \left[\frac{\partial S}{\partial X}\right]^T \left(-\frac{V_O}{L}(1-U) + \frac{V_{PV}}{L}\right) \tag{4.17}$$

The first term of the Equation 4.17 is presented as follows:

$$\left[\frac{\partial S}{\partial I_{PV}}\right] = \frac{1}{V_{PV}} - \frac{I_{PV}}{V_{PV}^2}\frac{\partial V_{PV}}{\partial I_{PV}} + \frac{1}{aV_{th}}\frac{\partial V_{PV}}{\partial I_{PV}}\frac{\partial I_{PV}}{\partial V_{Pv}} \tag{4.18}$$

The calculation of the derivative of the current I_{PV} with respect to the voltage indicates that this derivative is consistently negative:

$$\left[\frac{\partial I_{PV}}{\partial V_{PV}}\right] = -\frac{1}{aV_{th}} I_O \exp\left(\frac{V_{PV}}{aV_{th}}\right) < 0 \tag{4.19}$$

Additionally, the derivative of the voltage V_{PV} with respect to the current is consistently negative:

$$\frac{\partial V_{PV}}{\partial I_{PV}} q = -aV_{th}\left(\frac{I_O}{I_{ph} + I_D - I_{PV}}\right) \tag{4.20}$$

After performing these operations, the sign of the Equation 4.17 is determined to be positive, specifically $\frac{\partial S}{\partial I_{PV}}$, so the parameters λ_1, λ_2, and λ_3 must be positives.

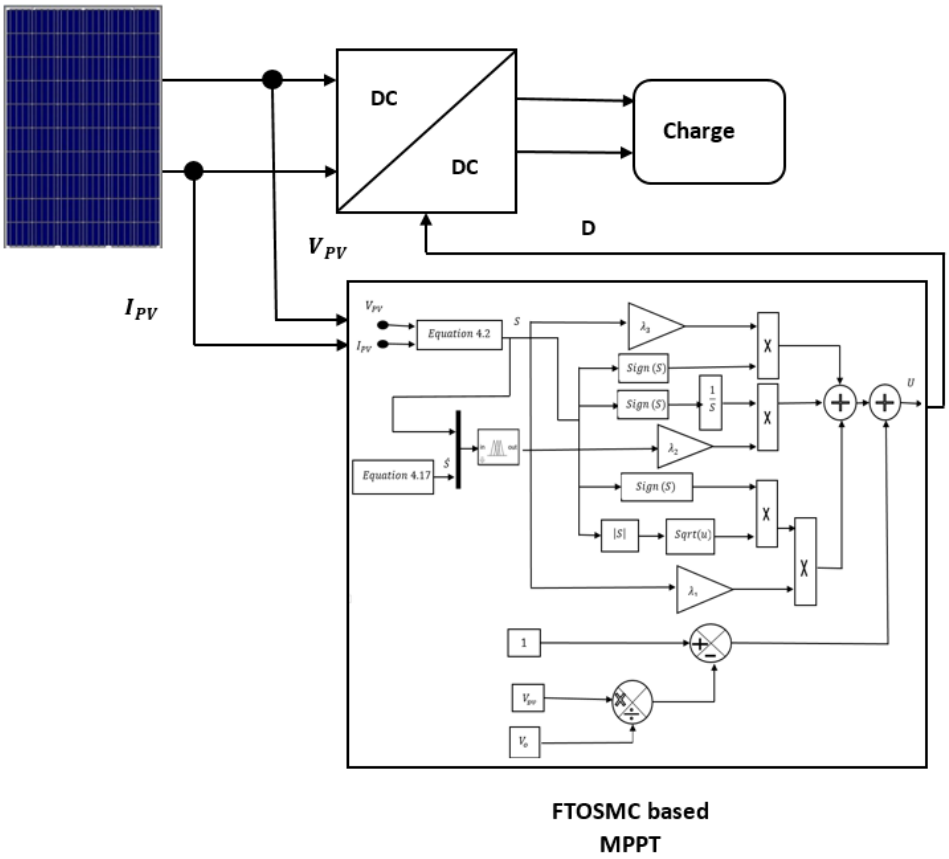

Figure 5. PVS scheme.

5. Proposed FTOSMC

The fuzzy logic controller (FLC) has attracted significant interest from researchers and has been applied across various fields. By leveraging fuzzy logic, an FLC processes data and conditions in a more flexible and intelligent manner compared to conventional binary logic [23, 26]. It is widely utilized in areas such as process control, communication, business, medicine, and more. However, the majority of research in fuzzy logic has primarily focused on control systems.

In this work, we introduce a Mamdani FLC designed to tune the switching gain in TOSMC, aiming to reduce the chattering phenomenon. The controller features two inputs (error and change in error) and a single output, which represents the duty cycle value.The fuzzy logic rules, are utilized to dynamically adjust the switching gain to achieveoptimal performance. The switching gain, λ, is based on the value of the sliding surface S. Therefore, the updated gain of the control algorithm will be:

$$\lambda_1' = \lambda_1 \times U \tag{5.1}$$

$$\lambda_2' = \lambda_2 \times U \tag{5.2}$$

$$\lambda_3' = \lambda_3 \times U \tag{5.3}$$

6. Simulation and results

To evaluate the effectiveness and suitability of the proposed FTOSMC for MPPT, simulations were conducted under varying solar irradiation conditions, including both real and typical solar irradiation profiles.

The proposed MPPT system was implemented and simulated using MATLAB/Simulink.First, a conventional DC-DC boost converter was modeled and connected to a PV array. The key parameters of the PV system are detailed in Table III (Appendix). A load was then connected to the output of the converter, as illustrated in Figure 5.

The FTOSMC controller introduces a fuzzy logic layer to the conventional TOSMC structure. Its purpose is to dynamically tune the control gain according to the system state, thereby reducing the chattering commonly observed in classical SMC and TOSMC. By analyzing the output power and tracking performance, it is evident that the fuzzy system significantly improves the convergence speed to the maximum power point while maintaining a smooth and stable output. This effect is particularly visible in the comparative simulations, where the FTOSMC demonstrates superior behavior under both typical and real conditions, as shown in Figures 13 and 14.

In addition, the fuzzy logic rules (Table I) are designed to increase the control gain when the system is far from equilibrium and reduce it when the sliding surface approaches zero, achieving a balance between fast tracking and reduced switching activity. This adaptive mechanism is key to the performance of FTOSMC and has been validated through simulation results.

Simulations were carried out under two different operating conditions:

- **Case 1:** Typical solar irradiation and temperature profiles (Figures 6 and 7).
- **Case 2:**Real solar irradiation profile (Figures 11 and 12).

To ensure the converter operates in continuous conduction mode (CCM), its parameters were selected to exceed the minimum threshold values dictated by standard design equations. The detailed component values of the boost converter are provided in Table II (Appendix).

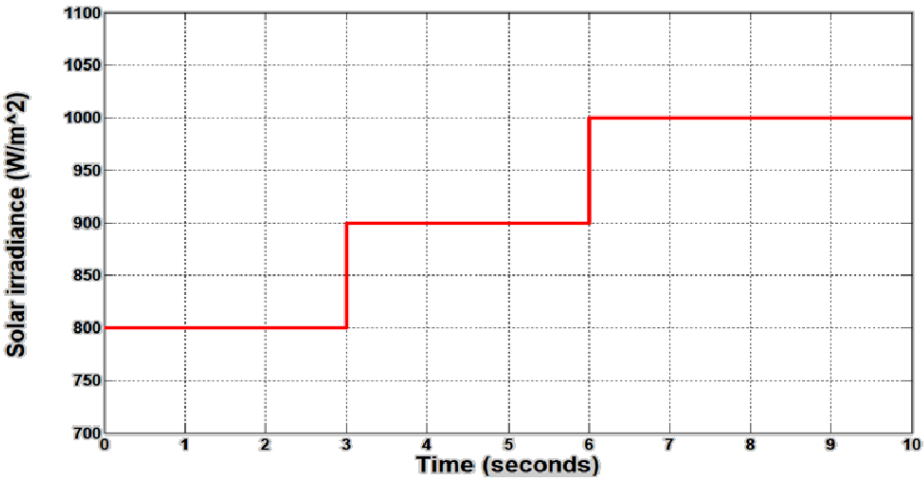

Figure 6. Solar insolation profile.

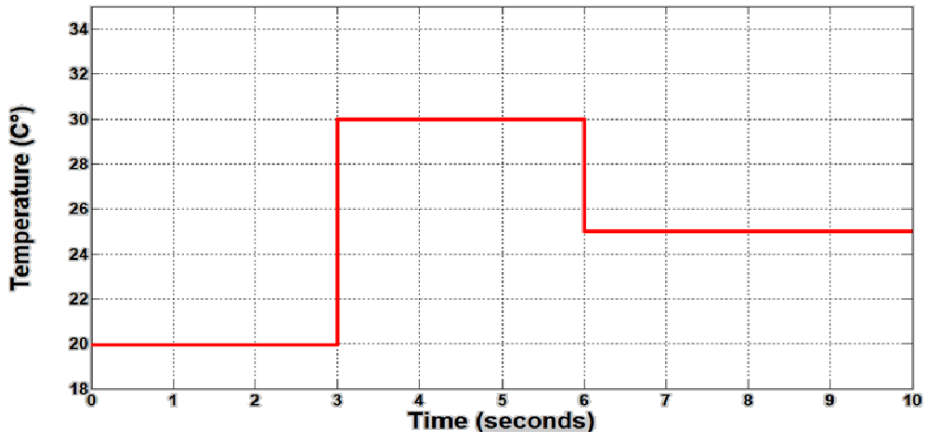

Figure 7. Temperature profile.

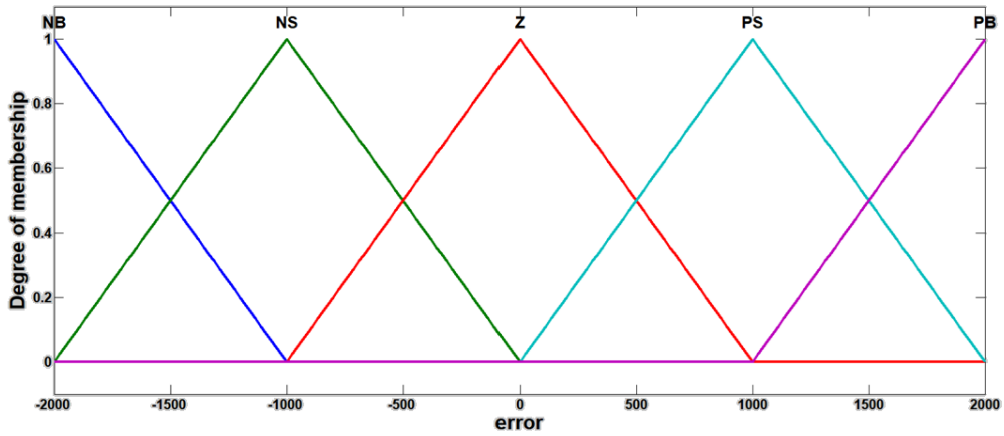

Figure 8. Input 1 membership-function.

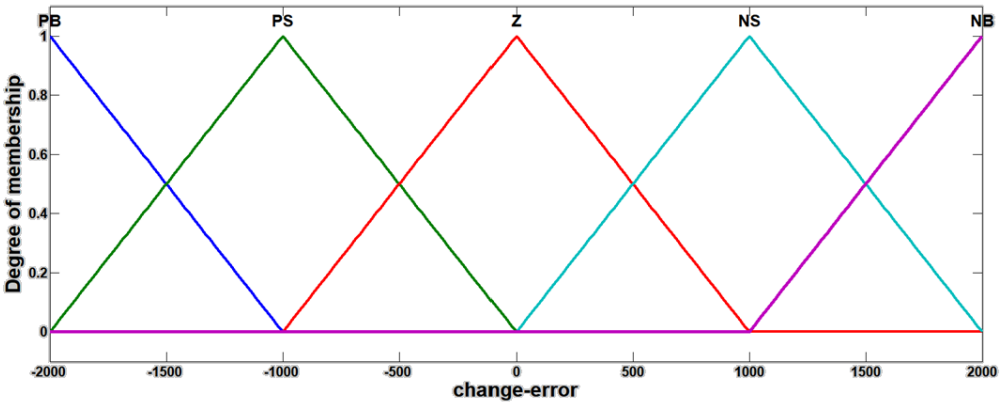

Figure 9. Input 2 membership-function.

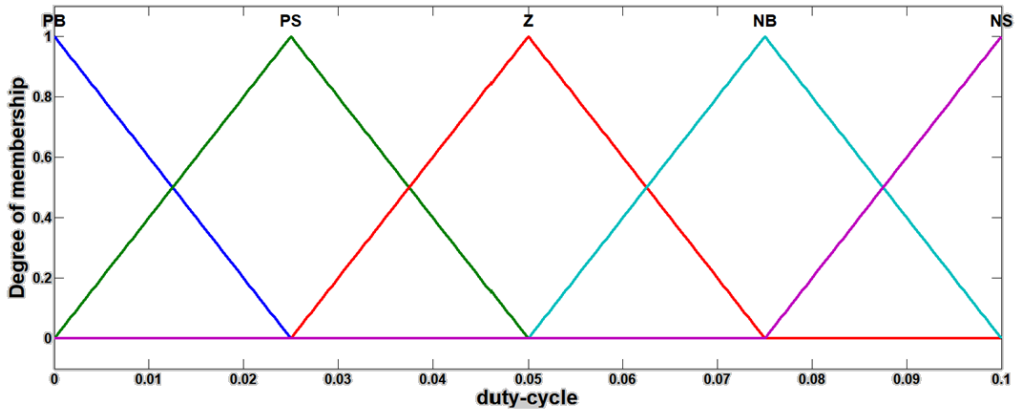

Figure 10. Output membership-function.

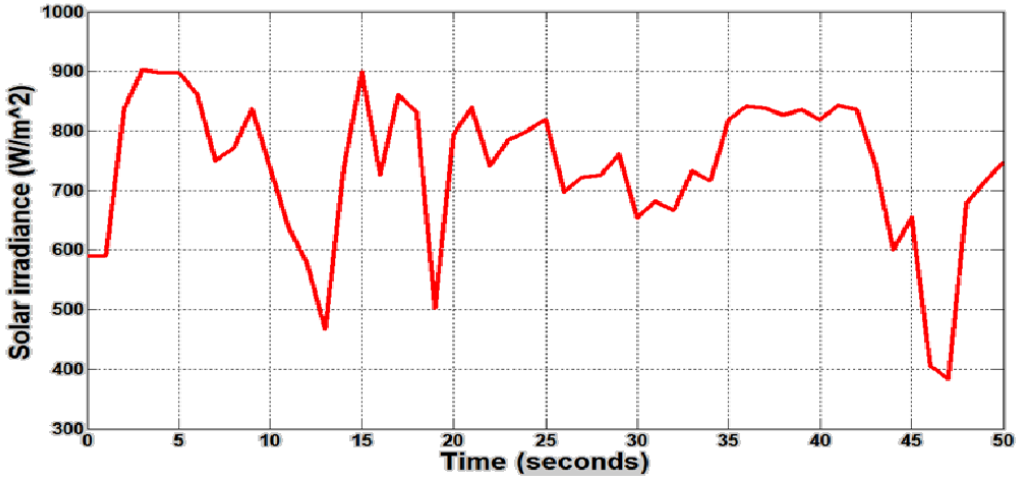

Figure 11. Reel solar insolation profile.

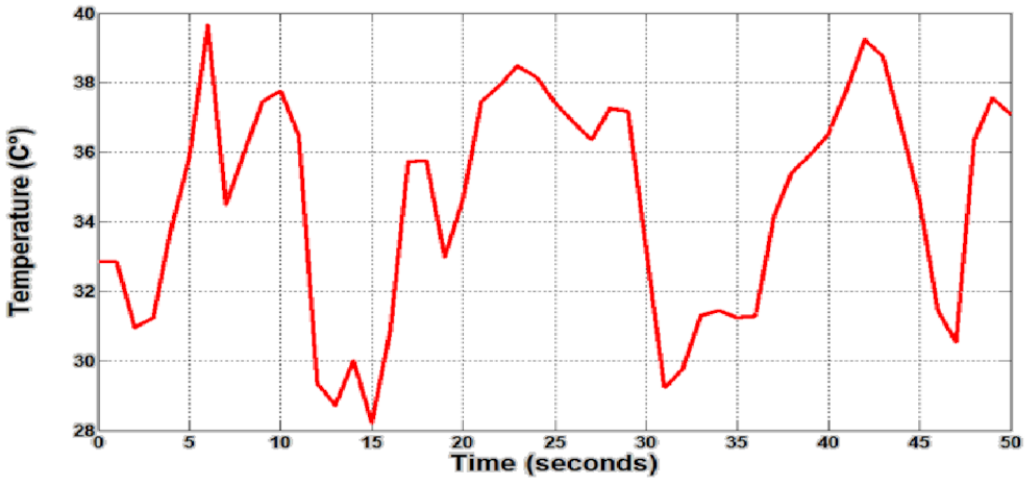

Figure 12. Reel temperature profile.

The boost converter is controlled using the proposed FTOSMC strategy, where the fuzzy logic rules governing the control mechanism are comprehensively detailed in Table I (Appendix). The two inputs and the output of the fuzzy control system are illustrated in Figures 8, 9, and 10, providing insight into the control logic and its impact on system performance.

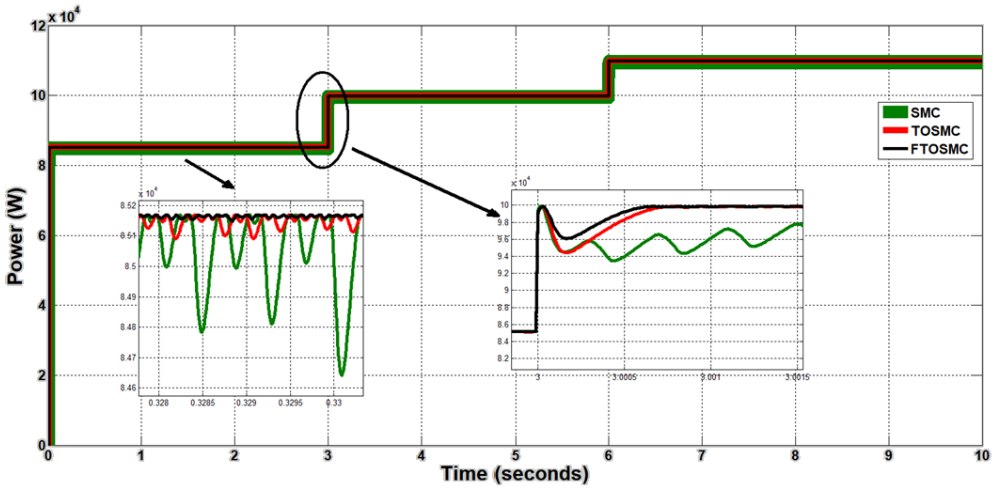

Figure 13. Output power of PV array for typical profile.

The output power delivered to the load is shown in Figure 13 for the typical profile and in Figure 14 for the real profile. To assess the robustness of the proposed FTOSMC strategy, a comparative analysis was conducted against both the standard SMC and the TOSMC, as depicted in Figure 4. The results demonstrate that the proposed FTOSMC significantly reduces power output chattering compared to both SMC and TOSMC. This confirms its superior robustness under fluctuating temperature and irradiance conditions. Additionally, the FTOSMC ensures faster convergence to the maximum power point while maintaining high efficiency and smooth power delivery, making it particularly suitable for standalone PV applications.

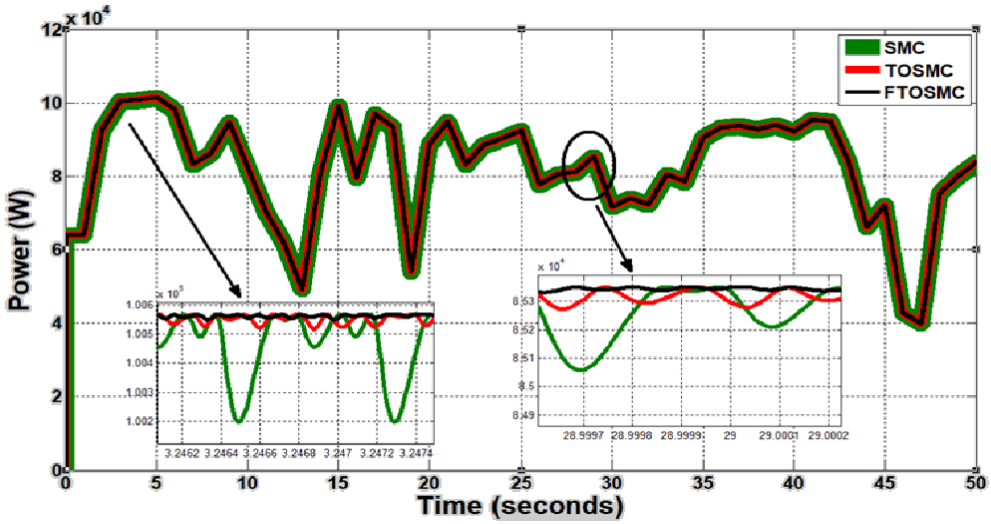

Figure 14. Output power of PV array for reel profile.

7. Conclusions

This study looks at using a FTOSMC to maximize solar power for a PV panel. A DC-DC boost converter is used for this purpose. Therefore, efficiency and accuracy can be improved by minimizing transients and reducing deviations from the peak power point. Our research discovered that the FTOSMC outperforms the others to control the DC/DC boost converter in an uncertain environment to deliver maximum power point. To effectively track the power output of a PV array operating under various conditions, this paper proposes the use of a FTOSMC.

The simulation results, conducted across three different scenarios—case 1 with reel profile of irradiance and temperature, case 2 with typical profile of irradiance and temperature, demonstrate that the proposed method can successfully control power output while ensuring convergence to the maximum power point (MPP).

For future work, the integration of Type-2 uzzy logic in the FTOSMC framework will be explored to further enhance robustness against uncertainties and external disturbances. Additionally, real-time hardware implementation and the extension of this controller to hybrid PV-battery energy storage systems will be investigated to assess its practical feasibility.

Author contributions

Nesrine Cherigui carried out the simulations, contributed to the modeling of the system, and wrote the first version of the manuscript. Abdelkarim Chemidi conceived the main idea, performed the corrections, and contributed to the analysis and interpretation of the results. Ahmad Tahour revised the manuscript critically for technical and scientific content and helped improve the overall structure and clarity of the paper. Mohamed Horch assisted in the analysis of the results. All authors reviewed and approved the final version of the manuscript.

Use of Generative-AI tools declaration

The authors declare they have used Artificial Intelligence (AI) tools in the creation of this article.

Conflict of interest

All authors declare no conflicts of interest in this paper.

References

1. Althobaiti A, Ullah N, Belkhier Y, Jamal Babqi A, Alkhammash HI, Ibeas A (2023) Expert knowledge based proportional resonant controller for three phase inverter under abnormal grid conditions. *International Journal of Green Energy* 20: 767–783. https://doi.org/10.1080/15435075.2022.2107395
2. Ullah N, Sami I, Jamal Babqi A, Alkhammash HI, Belkhier Y, Althobaiti A, et al. (2023) Processor in the loop verification of fault tolerant control for a three phase inverter in grid connected pv

system. *Energy Sources, Part A: Recovery, Utilization, and Environmental Effects* 45: 3760–3776. https://doi.org/10.1080/15567036.2021.2015486

3. Katche ML, Makokha AB, Zachary SO, Adaramola MS (2023) A comprehensive review of maximum power point tracking (mppt) techniques used in solar pv systems. *Energies* 16: 2206. https://doi.org/10.3390/en16052206
4. Başoğlu ME (2022) Comprehensive review on distributed maximum power point tracking: Submodule level and module level mppt strategies. *Solar Energy* 241: 85–108. https://doi.org/10.1016/j.solener.2022.05.039
5. Ali Z, Abbas SZ, Mahmood A, Ali SW, Javed SB, Su CL (2023) A study of a generalized photovoltaic system with mppt using perturb and observer algorithms under varying conditions. *Energies* 16: 3638. https://doi.org/10.3390/en16093638
6. Sadick A (2023) Maximum power point tracking simulation for photovoltaic systems using perturb and observe algorithm. https://doi.org/10.5772/intechopen.111632
7. John R, Mohammed SS, Zachariah R (2017) Variable step size perturb and observe mppt algorithm for standalone solar photovoltaic system. In *2017 IEEE International Conference on Intelligent Techniques in Control, Optimization and Signal Processing (INCOS)*, 1–6. IEEE. https://doi.org/10.1109/ITCOSP.2017.8303163
8. Bakar Siddique MA, Asad A, Asif RM, Rehman AU, Sadiq MT, Ullah I (2023) Implementation of incremental conductance mppt algorithm with integral regulator by using boost converter in grid-connected pv array. *IETE Journal of Research* 69: 3822–3835. https://doi.org/10.1080/03772063.2021.1920481
9. Yılmaz M, Corapsiz M (2022) Artificial neural network based mppt algorithm with boost converter topology for stand-alone pv system. *Erzincan University Journal of Science and Technology* 15: 242–257. https://doi.org/10.18185/erzifbed.1002823
10. Ullah K, Ishaq M, Tchier F, Ahmad H, Ahmad Z (2023) Fuzzy-based maximum power point tracking (mppt) control system for photovoltaic power generation system. *Results in Engineering* 20: 101466. https://doi.org/10.1016/j.rineng.2023.101466
11. Babaie M, Sharifzadeh M, Mehrasa M, Chouinard G, Al-Haddad K (2020) Pv panels maximum power point tracking based on ann in three-phase packed e-cell inverter. In *2020 IEEE International Conference on Industrial Technology (ICIT)*, 854–859. IEEE. https://doi.org/10.1109/ICIT45562.2020.9067218
12. Abouzeid AF, Eleraky H, Kalas A, Rizk R, Elsakka MM, Refaat A (2024) Experimental validation of a low-cost maximum power point tracking technique based on artificial neural network for photovoltaic systems. *Scientific Reports* 14: 18280. https://doi.org/10.1038/s41598-024-67306-0
13. Chou KY, Yeh YW, Chen YT, Cheng YM, Chen YP (2020) Adaptive neuro fuzzy inference system based mppt algorithm applied to photovoltaic systems under partial shading conditions. In *2020 International Automatic Control Conference (CACS)*, 1–6. IEEE. https://doi.org/10.1109/CACS50047.2020.9289733
14. Vo TH (2023) Design of the adaptive neuro-fuzzy inference system (anfis) and a genetic algorithm controller for solar photovoltaic systems using the boost converter. *Journal of Technical Education Science* 18: 109–118. https://doi.org/10.54644/jte.78A.2023.1439

15. Dkhichi F (2023) Improved mppt algorithm: Artificial neural network trained by an enhanced gauss-newton method. *AIMS Electronics & Electrical Engineering* 7: 380–405. https://doi.org/10.3934/electreng.2023020

16. Obukhov S, Ibrahim A, Diab AAZ, Al-Sumaiti AS, Aboelsaud R (2020) Optimal performance of dynamic particle swarm optimization based maximum power trackers for stand-alone pv system under partial shading conditions. *IEEE Access* 8: 20 770–20 785. https://doi.org/10.1109/ACCESS.2020.2966430

17. Dagal I, Akın B, Akboy E (2022) Mppt mechanism based on novel hybrid particle swarm optimization and salp swarm optimization algorithm for battery charging through simulink. *Scientific reports* 12: 2664. https://doi.org/10.1038/s41598-022-06609-6

18. Belmadani H, Bradai R, Kheldoun A, Mohammed KK, Mekhilef S, Belkhier Y, et al. (2024) A new fast and efficient mppt algorithm for partially shaded pv systems using a hyperbolic slime mould algorithm. *International Journal of Energy Research* 2024: 5585826. https://doi.org/10.1155/2024/5585826

19. Messaoudi F, Farhani F, Zaafouri A (2024) A new approach to mppt hybrid incremental conductance-sliding mode control for pv grid-connected. *Measurement and Control* 57:1370–1382. https://doi.org/10.1177/00202940241240666

20. Benbouhenni H, Bizon N (2021) Third-order sliding mode applied to the direct field-oriented control of the asynchronous generator for variable-speed contra-rotating wind turbine generation systems. *Energies* 14: 5877. https://doi.org/10.3390/en14185877

21. Bouhadji F, Bouyakoub I, Mehedi F, Kacemi WM, Reguieg Z (2024) Optimization of grid power quality using third order sliding mode controller in pv systems with multilevel inverter. *Energy Reports* 12: 5177–5193. https://doi.org/10.1016/j.egyr.2024.10.064

22. Hassan Q, Viktor P, Al-Musawi TJ, Ali BM, Algburi S, Alzoubi HM, et al. (2024) The renewable energy role in the global energy transformations. *Renewable Energy Focus* 48: 100545. https://doi.org/10.1016/j.ref.2024.100545

23. Manuel NL, İnanç N (2022) Sliding mode control-based mppt and output voltage regulation of a stand-alone pv system. *Power Electronics and Drives* 7: 159–173. https://doi.org/10.2478/pead-2022-0012

24. Heydari M, Heydari A, Amini M (2023) Solar power generation and sustainable energy: a review. *International Journal of Technology and Scientific Research* 12: 342–349.

25. Zhang Y, Wang YJ, Yu JQ (2022) A novel mppt algorithm for photovoltaic systems based on improved sliding mode control. *Electronics* 11: 2421. https://doi.org/10.3390/electronics11152421

26. Jamshidi F, Salehizadeh MR, Yazdani R, Azzopardi B, Jately V (2023) An improved sliding mode controller for mpp tracking of photovoltaics. *Energies* 16: 2473. https://doi.org/10.3390/en16052473

Appendix

Table 1. Fuzzy control rules.

	Fuzzy rules					
error		NB	NS	Z	PS	PB
Change in error	PB	Z	PS	PS	PB	PB
	PS	PS	Z	PS	PS	PB
	Z	PS	PS	Z	PS	PS
	NS	PB	PS	PS	Z	PS
	NB	PB	PB	PS	PS	Z

Table 2. The components of converter and parameters.

Components and parameters	**Value**
Inductor	5 mH
Forward voltage V_f of Diode	0.8 V
Output capacitor	6000 F
Switching frequency (KHZ)	5 KHZ

Table 3. The parameters of PV array.

Parameter	**Value**
Maximum Power (W)	100000
Cells per Module (N_{cell})	96
Open circuit voltage V_{OC} (V)	64.2
Short circuit current I_{sc} (A)	5.96
Voltage at MPP V_{MP} (V)	54.7
Current at MPP I_{MP} (A)	5.58
Temperature (°C)	25
Parallel string (N_p)	60
Series connected modules per string (N_a)	6